Crystal-induced and image-potential-induced empty surface states on Cu(111) and Cu(001)

S. L. Hulbert and P. D. Johnson
Physics Department, Brookhaven National Laboratory, Upton, New York 11973

N. G. Stoffel, W. A. Royer, and N. V. Smith
AT&T Bell Laboratories, Murray Hill, New Jersey 07974
(Received 21 January 1985)

Empty surface states of both the crystal-induced and image-potential-induced kinds have been observed on Cu(111) using k-resolved inverse photoemission. Measurements were performed at $\hbar\omega = 10.2$ and 11.0 eV using a novel refracting monochromator. A simplified application of multiple-reflection theory explains the binding energies, establishes the relationship between the two kinds of state, and shows how these depend on crystal face.

Empty surface states are now accessible for study using k-revolved inverse photoemission spectroscopy (KRIPES). It becomes necessary, however, to consider the special class of surface states which arise through the long-range nature of the image-potential barrier.[1] This is in contrast to ordinary photoemission where one sees filled surface states, and these are invariably "crystal induced" in the sense that they are intimately connected with the properties of bulk band structure. In this paper we report KRIPES measurements on Cu(111) in which we observe on the same sample *both* the crystal-induced *and* image-potential-induced surface states. We show how their relationship, their binding energy, and its crystal-face dependence can all be understood in terms of a simple scheme based on the multiple-reflection formalism for surface states.[2,3]

Our experimental apparatus incorporates a BaO-cathode electron gun which has been specifically designed for low energy and high brightness in the space-charge-limited region[4] giving a momentum resolution of 0.1 Å^{-1}. Photon detection and analysis are accomplished using a novel, yet remarkably simple, refracting monochromator based on the strong chromatic aberration of a LiF lens.[5] The overall layout is shown in Fig. 1. Its theoretical resolution function is given by $\Delta\hbar\omega/\hbar\omega \simeq p_0/a_0$ where p_0 and a_0 are the respective diameters of the pinhole and lens apertures ($a_0 = 90$ mm, $p_0 = 2.5$ mm in the present case). Overall resolution, including the electron source, is ~ 0.7 eV. The instrument offers tunability of $\hbar\omega$ (longitudinal dispersion $= 128$ mm eV^{-1}) by scanning the pinhole along the main axis. The sample was cleaned and characterized using the standard techniques of low-energy electron diffraction (LEED) and Auger electron spectroscopy (AES).

Figure 2 shows our KRIPES measurements on Cu(111) at $\hbar\omega = 10.2$ eV as a function of the angle of electron incidence θ_e. At $\theta_e \simeq 10°$ a prominent peak appears at the Fermi level E_F and then disperses upward with increasing θ_e. We identify this as the continuation above E_F of the well known and well established[6–8] occupied surface state first seen in photoemission by Gartland and Slagsvold.[6] At $\theta_e \approx 45°$ another prominent peak appears at E_F which (as shown below) is readily explicable as a direct transition within the bulk band structure.

At normal incidence $\theta_e = 0°$ we observe a distinct peak at 0.94 eV below the vacuum level E_V. We identify this as the $n = 1$ component of a Rydberg series of image-potential surface states similar to those which have been reported previously on a number of other crystal surfaces.[1,9–11] The binding energy is obtained by taking E_F at the peak of the Gartland-Slagsvold state at the extrapolated angle of crossover from the occupied to unoccupied regions, and by taking the work function of Cu(111) to be 4.94 eV.[12] The estimated limits of error on the binding energy are ± 0.15 eV.

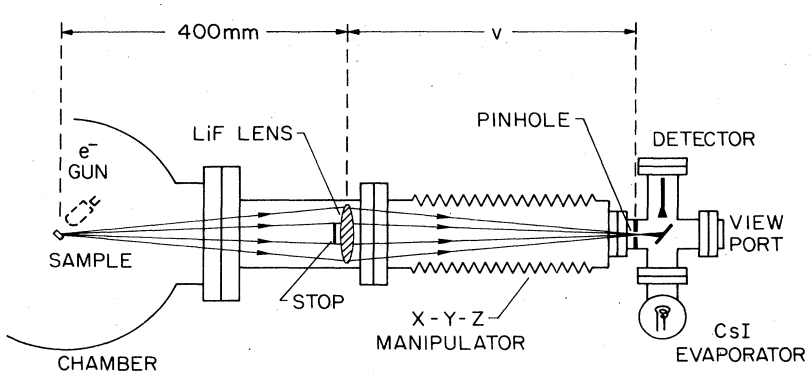

FIG. 1. Layout of the apparatus showing the relative positions of the sample, electron gun, and LiF-lens monochromator. (The detection manifold has been rotated 90° about the main axis.)

 ©1985 The American Physical Society

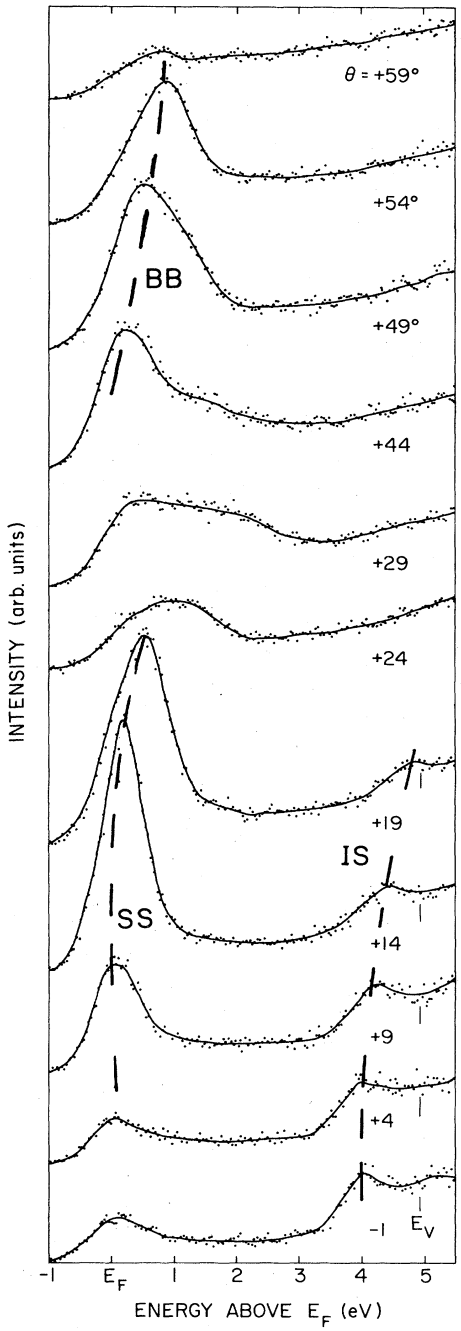

FIG. 2. KRIPES data on Cu(111) taken as a function of electron incidence angle in the $\bar{\Gamma}\bar{K}$ azimuth at $\hbar\omega = 10.2$ eV.

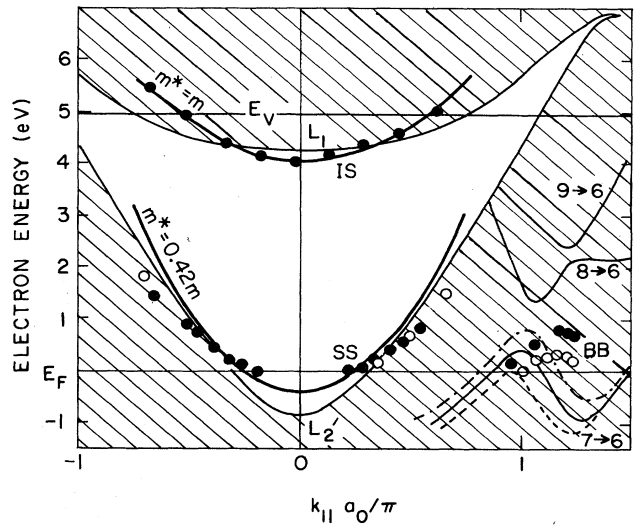

FIG. 3. Experimental and theoretical $E(k_{\parallel})$ dispersion relations. Filled and open circles correspond to data taken at $\hbar\omega = 10.2$ and 11.0 eV, respectively. Crosshatched area is the projection of the bulk band structure. The crystal-induced surface state (SS) follows closely a $m^* = 0.42$-m dispersion. The image-potential states (IS) follow a free-electron ($m^* = m$) dispersion. The bulk band-structure feature (BB) falls close to predictions based on direct transitions between bands $7 \rightarrow 6$ (solid curves are for $\hbar\omega = 10.2$ eV; dash-dot and dashed curves are for $\hbar\omega = 9.4$ and 11.0 eV, respectively). a_0 is the lattice parameter ($= 3.615$ Å).

Experimental $E(k_{\parallel})$ relations obtained at $\hbar\omega = 10.2$ and 11.0 eV are compared with theory in Fig. 3. At E_F, the crystal-induced surface state (SS) falls close to the continuation of the parabolic dispersion relation ($m^* = 0.42m$) determined below E_F by Kevan[8] using high precision angle-resolved photoemission. On increasing $k_{\parallel}$ the SS peak appears to fall below the parabola and to merge with the bulk continuum becoming a surface resonance. The image-potential state (IS) displays a free-electron-like ($m^* = m$) dispersion. The bulk-band-structure feature (BB) which appears fleetingly near $k_{\parallel} = \pi/a_0$ is nicely accounted for by theoretical calculations based on bulk direct transitions.[13]

Both kinds of states are generated theoretically in the surface scattering formalism[2,3] which pictures electron waves being repeatedly reflected between the bulk crystal and the image-potential barrier. If we denote the respective reflectivities by $r_C e^{i\phi_C}$ and $r_B e^{i\phi_B}$, bound states correspond to the poles of the function

$$\psi_+ = \{1 - r_C r_B \exp[i(\phi_C + \phi_B)]\}^{-1} , \quad (1)$$

and occur when the total phase

$$\phi \equiv \phi_C + \phi_B = 2\pi n, \quad n = 1, 2 \ldots . \quad (2)$$

Crystal-induced surface states are those determined by the behavior of ϕ_C. This category would include all surface states observed in ordinary photoemission and also those generated in typical theoretical calculations. On approaching the vacuum level E_V, ϕ is dominated by the behavior of ϕ_B which, because of the *long-range* nature of the image potential, diverges according to the formula[2]

$$\phi_B/\pi = [(3.4 \text{ eV})/(E_V - E)]^{1/3} - 1 . \quad (3)$$

Thus, the condition of Eq. (2) can be satisfied *ad infinitum,* giving rise to a Rydberg series. If ϕ_C can be treated as constant over the energy range of the series, the binding energies at $k_{\parallel} = 0$ can be expressed by the simple formula $e_n = (0.85 \text{ eV})/(n + a)^2$ where the quantum defect $a \equiv \frac{1}{2}(1 - \phi_C/\pi)$.

There has been some discussion on where one should start enumerating the surface states,[1,11] and on how one should accommodate the crystal-induced state into the

scheme. We shall adopt here a simple scheme in which the crystal-induced surface state will emerge at the "$n=0$" level.

The energy dependence (at $k_{\parallel}=0$) of the phases ϕ_C, ϕ_B, and ϕ for Cu(111) is shown in Fig. 4(a). The $L_{2'} \rightarrow L_1$ gap is "Shockley inverted" in that the p-like $L_{2'}$ level lies below the s-like L_1 level. The phase ϕ_C increases from 0 to π across such a gap, and its functional form has been evaluated using a simple nearly free-electron formula.[14] ϕ_B is obtained from Eq. (3). The predicted binding energy for the $n=1$ image state is $e_1=0.8$ eV in reasonable accord with the observed value of 0.94 ± 0.15 eV. Proceeding to lower energies, ϕ passes through 0 at $E=E_F-0.5$ eV, in good agreement with the $k_{\parallel}=0$ location of the crystal-induced surface state—hence, our "$n=0$" designation of this state.

The extension of this argument to Cu(001) is illustrated in Fig. 4(b). The Shockley-inverted $X_{4'} \rightarrow X_1$ gap lies higher than in Cu(111), and E_V falls about midgap. The predicted value for e_1 is 0.55 eV, which agrees reasonably well with the reported experimental value[10] of 0.64 eV. We have confirmed this value in the present apparatus using the same procedure described above (work function 4.59 eV, Ref. 12).

The important point is that the theoretical e_1 is smaller on Cu(001) than on Cu(111) and this is simply related to the behavior of ϕ_C. For Cu(111), E_V lies above the top of the bulk band gap, so that ϕ_C has accumulated just about all of its π increment. For Cu(001), E_V falls midgap so that ϕ_C has accumulated only about half this value. Indeed, if we fit ϕ_C (or, equivalently, the quantum defect a) to the measured binding energies we obtain $\phi_C=1.1\pi$ and 0.7π for Cu(111) and Cu(001), respectively, differing by roughly $\pi/2$ as expected. [The image-potential states observed on Ni(001),[1] Pd(111),[11] and Au(001) (Ref. 10) also fall in midgap and have e_1 close to 0.6 eV corresponding to $\phi_C \approx \pi/2$.] We conclude that the observed difference between e_1 for the (111) and (001) faces of Cu appears to be real and that it follows from the relative position of E_V with respect to the bulk band gap.

Extrapolating the phase ϕ to lower energies for Cu(111) gives excellent agreement for the energy of the crystal-induced surface state if we designate it as the $n=0$ level. To complete the picture we require [see Fig. 4(b)] on Cu(001) the existence of a surface *resonance* lying a few tenths of an eV below the $X_{4'}$ band edge. Evidence for such a resonance appears as a weak shoulder or asymmetry on a much stronger peak due to bulk direct transitions.[9,15]

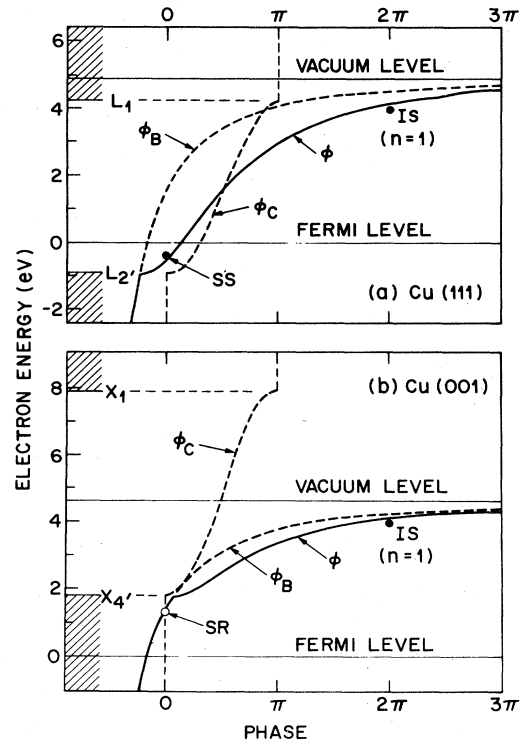

FIG. 4. Energy variation of the phases ϕ_C, ϕ_B, and ϕ showing the $n=1$ image-potential states (IS) and (a) the "$n=0$" crystal-induced state (SS) for Cu(111), (b) the proposed "$n=0$" surface resonance (SR) for Cu(001).

In conclusion, a rather simple phase analysis has yielded two new insights. Firstly, we have established both experimentally and theoretically the relationship and distinction between crystal-induced and image-potential-induced surface states. Secondly, we have shown how this relationship depends on the crystal face.

The work at Brookhaven was supported by the U.S. Department of Energy under Contract No. DE-AC02-76CH00016.

[1]P. D. Johnson and N. V. Smith, Phys. Rev. B **27**, 2527 (1983).
[2]E. G. McRae, Rev. Mod. Phys. **51**, 541 (1979).
[3]P. M. Echenique and J. B. Pendry, J. Phys. C **11**, 2065 (1978).
[4]N. G. Stoffel and P. D. Johnson, Nucl. Instrum. Methods (to be published).
[5]T. T. Childs, W. A. Royer, and N. V. Smith, Rev. Sci. Instrum. (to be published).
[6]P. O. Gartland and B. J. Slagsvold, Phys. Rev. B **12**, 4047 (1975).
[7]P. Heimann, J. Hermanson, H. Miosga, and H. Neddermeyer, Surf. Sci. **85**, 263 (1979).
[8]S. D. Kevan, Phys. Rev. Lett. **50**, 526 (1983).
[9]V. Dose, W. Altmann, A. Goldmann, U. Kolac, and J. Rogozik, Phys. Rev. Lett. **52**, 1919 (1984).
[10]D. Straub and F. J. Himpsel, Phys. Rev. Lett. **52**, 1922 (1984).
[11]D. A. Wesner, P. D. Johnson, and N. V. Smith, Phys. Rev. B **30**, 503 (1984). This paper reports image-potential states on Pd(111) and withdraws an earlier claim to have observed crystal-induced surface states on this surface: P. D. Johnson and N. V. Smith, Phys. Rev. Lett. **49**, 290 (1982).
[12]P. O. Garland, Phys. Norv. **6**, 201 (1972).
[13]N. V. Smith, Phys. Rev. B **19**, 5019 (1979).
[14]E. T. Goodwin, Proc. Cambridge Philos. Soc. **35**, 205 (1939).
[15]D. P. Woodruff, N. V. Smith, P. D. Johnson, and W. A. Royer, Phys. Rev. B **26**, 2943 (1982); D. P. Woodruff, S. L. Hulbert, P. D. Johnson, N. G. Stoffel, and N. V. Smith (unpublished).